AN INFINITE, CONVERGING, SEQUENCE OF BROCARD PORISMS

DAN REZNIK AND RONALDO GARCIA

ABSTRACT. The Brocard porism is a 1d family of triangles inscribed in a circle and circumscribed about an ellipse. Remarkably, the Brocard angle is invariant and the Brocard points are stationary at the foci of the ellipse. In this paper we show that a certain derived triangle spawns off a second, smaller, Brocard porism so that repeating this calculation yields an infinite, converging sequence of porisms. We also show that this sequence is embedded in a continuous family of porisms.

Keywords Poncelet, Brocard, Porism, Locus, Invariant, Envelope, Recurrence, Nesting, Convergence

 \mathbf{MSC} 53A04 and 51M04 and 51N20

1. Introduction

The Brocard points Ω_1 , Ω_2 , shown in Figure 1 are well-studied, unique points of concurrence in a triangle, introduced by August L. Crelle in 1816, given a construction by Karl F.A. Jacobi in 1825, and rediscovered by Henri Brocard in 1875 [19, Brocard Points].

The Brocard *porism*, Figure 1, is a 1d family of Poncelet 3-periodics (triangles) inscribed in a circle and circumscribed about an ellipse \mathcal{E} known as the *Brocard*

Date: September, 2020.

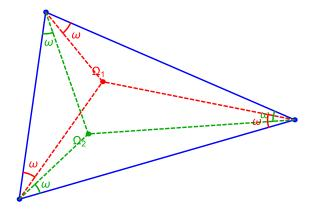


FIGURE 1. The Brocard Points Ω_1 (resp. Ω_2) are where sides of a triangle concur when rotated about each vertex by the Brocard angle ω . When sides are traversed and rotated clockwise (resp. counterclockwise), one obtains Ω_1 (resp. Ω_2).

(a,b)=(1.250,1.000), θ =25.0°, ω =23.5782°

FIGURE 2. A 3-periodic (blue) ABC in the Brocard Porism is shown inscribed in an external circle Γ (black) and the Brocard inellipse $\mathcal E$ (black). The tangency points are given by intersections D, E, F of symmedians (cevians through X_6) with the sidelengths. The Brocard points Ω_1, Ω_2 are stationary at the foci of $\mathcal E$. The Brocard circle $\mathcal K$ (green) contains Ω_1, Ω_2 , the circumcenter X_3 and the symmedian point X_6 , all of which are stationary. The center of $\mathcal K$ is X_{182} , the midpoint of X_3X_6 , aka the Brocard axis. Also shown (purple) is the second Brocard triangle T' = A'B'C' inscribed in $\mathcal K$ whose vertices lie at the intersections of the symmedians with $\mathcal K$. The first isodynamic point X_{15} is on the Brocard axis, is stationary, and common for both the original and the T' family. Video

Inellipse [4]. Remarkably, the Brocard angle ω is invariant and the Brocard points Ω_1 and Ω_2 are stationary at the foci of \mathcal{E} .

As a review, the circle \mathcal{K} which contains both Brocard points and the circumcenter X_3 is known as the Brocard *circle* [19]. The symmedian point X_6 also lies on \mathcal{K} and X_3X_6 is known as the Brocard *axis*. Notice that over the porism, all said points are stationary, and therefore so is \mathcal{K} .

At least seven Brocard $triangles^1$ are known (named 1st, 2nd, etc.) [7], deriving directly from $\Omega_{1,2}$, \mathcal{K} and related objects. It turns out the 1st, 2nd, 5th, and 7th Brocard triangles are inscribed in \mathcal{K} ; see this Video.

Here we focus on the *second* Brocard triangle, denoted T', whose vertices lie at the intersections of symmedians (cevians through the symmedian point X_6) with the Brocard circle [19, Second Brocard Triangle]; see Figure 2.

One first intriguing observation (proved below), unique to T', is that over the porism, its Brocard points Ω'_1 and Ω'_2 of T' are also stationary; see Figure 3 and this Video. In turn, this leads to a stream of interesting properties.

Main results.

- The T' are 3-periodics of a second Brocard porism inscribed in \mathcal{K} and circumscribed about a smaller, less eccentric ellipse \mathcal{E}' .
- Recursive calculation of T' spawns an infinite sequence of ever-shrinking porisms which converge to the first isodynamic point X15 [19, Isodynamic

 $^{^{1}\}mathrm{The}$ 7th Brocard triangle was proposed during the course of this research.

Points], common to all families. Successive Brocard points lie on two circular arcs.

- Recursive calculation of the *inverse* 2nd Brocard triangles (denoted T^*) converges to a segment between two fixed points P_2, U_2 known as the Beltrami points [11].
- Sequential Brocard circles $\mathcal{K}, \mathcal{K}', \mathcal{K}'', \dots$ are nested within each other like a Russian doll.
- The discrete sequence of porisms is embedded in a continuous family where
 T' (and its inverse) can be regarded as operators which induce discrete
 jumps.
- The envelope of ellipses in the continuous porism is an ellipse with the isodynamic points as foci.

Related Work. A construction for the Brocard porism is given in [2, Theorem 4.20, p. 129]. Equibrocardal (Brocard angle conserving) triangle families are studied in [9]. Bradley defines several conics associated to the Brocard porism [3]. Odehnal has studied loci of triangle centers for the poristic triangle family [14] identifying dozens of stationary triangle centers; similarly, Pamfilos proves properties of the family of triangles with fixed 9-point and circumcircle [15]. We have previously studied triangle center loci over selected triangle families [6, 17]. We have also analyzed the Brocard porism alongside the Poncelet homothetic family establishing a similarity link between the two [16].

Article Structure. in Section 2 we review definitions and prove basic Brocard relations required in further sections. In Section 3 we prove properties of the family of second Brocard triangles in a Brocard porism. In Section 3 we study the infinite, discrete sequence of porisms induced by iterative calculations of the second Brocard triangle. Finally, in Section 5 we specify how said sequence is embedded in a continuous one.

Appendix A provides explicit expressions for the vertices of an isoceles 3-periodic in the porism. Appendix B provides a 1d parametrization for any 3-periodic in the porism. Appendix C contains additional supporting relations required by some of our proofs. Finally, Appendix D tabulates most symbols used herein.

2. Properties of Brocard Porism Triangles

We adopt Kimberling's X_k notation for triangle centers, e.g., X_1 for the incenter, X_2 for the barycenter, etc. [10]. Assume that $X_3 = (0,0)$ is at the origin. Referring to Figure 1

Definition 1 (Brocard Points). Let a reference triangle have vertices ABC when traversed counterclockwise. The first Brocard point Ω_1 is where sides AB, BC, CA concur when rotated a special angle ω about A, B, C, respectively. The second Brocard point Ω_2 is defined similarly by a $-\omega$ rotation CB, BA, AC about C, B, A, respectively.

Referring to Figure 2:

Definition 2 (Brocard Circle). This is the circle \mathcal{K} through X_3 , and the Brocard points Ω_1, Ω_2 .

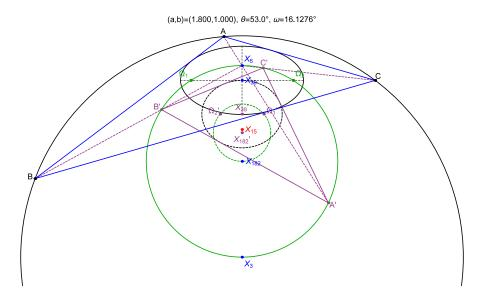


FIGURE 3. By construction (dashed purple), the second Brocard triangle T' (purple), is inscribed in the Brocard circle \mathcal{K} (green) of the its reference triangle T (blue). Remarkably, over the Brocard porism (outer circle, inner ellipse, both in solid black), the Brocard points $\Omega'_{2,1}$ of T' are also stationary. These coincide with the foci of a new, smaller, rounder, Brocard inellipse \mathcal{E}' (dashed black). The new, stationary, Brocard circle \mathcal{K}' (dashed green) is properly contained within \mathcal{K} . Notice the upper vertex of \mathcal{E}' coincides with the Brocard midpoint X_{39} of T. The isodynamic points X_{15}, X_{16} (latter not shown, above the page) are common and stationary for T and T'. Video

Note \mathcal{K} also contains X_6 , and it is centered on the midpoint X_{182} of X_3X_6 [19].

Referring to Figure 2:

Definition 3 (Brocard Porism). This is a 1d family of Poncelet 3-periodics inscribed in a circle of radius R (circumcenter X_3 is stationary) and circumscribed about an ellipse of semi-axes (a,b) known as the Brocard inellipse \mathcal{E} .

Over the family, the Brocard angle ω is invariant and the two Brocard points Ω_1 and Ω_2 are stationary at the foci of \mathcal{E} [4].

Corollary 1. Over the Brocard porism the Brocard circle and X_6 are stationary.

This stems from the fact that over the porism Ω_1, Ω_2, X_3 are stationary. Since X_6 is antipodal to X_3 on the so-called Brocard axis [19], it is also stationary. After [10]:

Definition 4 (Barycentric Combo). Let P and U be finite points on a triangle's plane with normalized barycentrics (p,q,r) and (u,v,w), respectively. Let f and g be homogeneous functions of the sidelengths. The (f,g) combo of P and U, also denoted f * P + g * U, is the point with barycentrics (f p + g u, f q + g v, f r + g w).

The Cyrillic letter u shall henceforth denote $\cot \omega$. Since $\omega \in [0, \pi/6]$ [19, Brocard Angle], then:

Remark 1. $w \ge \sqrt{3}$.

Lemma 1. Over the porism, the two Isodynamic points X_{15} and X_{16} are stationary and given by:

$$X_{15} = \left[0, \frac{R(\sqrt{3} - w)}{\sqrt{w^2 - 3}}\right], \quad X_{16} = \left[0, -\frac{R(\sqrt{3} + w)}{\sqrt{w^2 - 3}}\right]$$

Proof. Peter Moses (cited in [10, X(15), X(16)]) derives the following combos for the two isodynamic points:

(1)
$$X_{15} = \sqrt{3} * X_3 + u * X_6$$
$$X_{16} = \sqrt{3} * X_3 - u * X_6$$

With all involved quantities invariant, the result follows. Note that isodynamic points are self-inverses with respect to the circumcircle [19, Isodynamic Points]. For how we obtained the explicit expressions see Appendix $\mathbb C$.

Lemma 2. Let R and ω denote a triangle's circumradius and Brocard angle. The semi-axes (a,b) and center X_{39} of the Brocard inellipse \mathcal{E} are given by:

$$[a, b] = R \left[\sin \omega, 2 \sin^2 \omega \right] = R \left[\frac{1}{\sqrt{1 + u^2}}, \frac{2}{1 + u^2} \right]$$
$$X_{39} = \left[0, -\frac{Ru\sqrt{u^2 - 3}}{u^2 + 1} \right]$$

Proof. Consider a triangle T with sidelengths s_1, s_2, s_3 , area Δ , and circumradius R. The following identities appear in [4, 18]:

$$R = \frac{s_1 s_2 s_3}{4\Delta}, \quad \sin \omega = \frac{2\Delta}{\sqrt{\lambda}}, \quad |\Omega_1 - \Omega_2|^2 = 4c^2 = 4R^2 \sin^2 \omega (1 - 4\sin^2 \omega)$$

where $\lambda = (s_1 s_2)^2 + (s_2 s_3)^2 + (s_3 s_1)^2$ (named Γ in [18, Eqn. 2]), and $c^2 = a^2 - b^2$. The result follows from combining the above into the following expressions for the Brocard inellipse axes [19, Brocard Inellipse]:

$$a = \frac{s_1 s_2 s_3}{2\sqrt{\lambda}}, \qquad b = \frac{2s_1 s_2 s_3 \Delta}{\lambda}.$$

For how explicit expressions were obtained for X_{39} , see Appendix C.

Proposition 1. The circumradius R and w are given by:

$$R = \frac{2a^2}{b}, \quad u = \frac{\sqrt{4a^2 - b^2}}{b}.$$

Proof. Follows directly from Lemma 2.

Lemma 3. The coordinates for the symmedian point X_6 are given by:

$$X_6 = \left[0, -\frac{R\sqrt{u^2 - 3}}{u}\right]$$

A derivation is provided in Appendix C.

Corollary 2. The distance between circumcenter and symmedian point is given by

$$|X_3 - X_6| = \frac{R\sqrt{u^2 - 3}}{u}$$

Proposition 2. In terms of R and w, the Brocard points are given by:

$$\Omega_{1,2}(R, u) = \frac{R\sqrt{u^2 - 3}}{u^2 + 1} [\pm 1, -u]$$

Proof. Follows from Proposition 11 and Lemma 9.

Corollary 3. The center X_{39} of the Brocard inellipse \mathcal{E} is given by:

$$X_{39} = \left[0, -R \frac{w\sqrt{w^2 - 3}}{w^2 + 1} \right]$$

3. Properties of the family of second Brocard Triangles

Upwards of seven Brocard triangles are defined in [7]. The 1st, 2nd, 5th, and 7th Brocard triangles are inscribed in the Brocard circle, as shown on this video. Henceforth we shall focus on the second Brocard triangle, denoted T' = A'B'C'. All primed quantities $(\Omega'_i, \omega', \text{ etc.})$ below refer to those of T'. Specifically, X'_i stands for triangle center X_i of T'.

Referring to Figure 2:

Definition 5 (Second Brocard Triangle). The vertices A', B', C' of the second Brocard triangle T' lie at the intersections of cevians through X_6 with the Brocard circle \mathcal{K} , i.e., T' is inscribed in \mathcal{K} .

Over the Brocard porism:

Lemma 4. X'_3 (equivalent to X_{182}) is stationary and given by:

$$X_3' = X_{182} = \left[0, -\frac{R\sqrt{u^2 - 3}}{2u}\right]$$

This stems from the fact that T' is inscribed in fixed K whose center is X_{182} . The explicit formula is obtained by noting that X_{182} is the midpoint of X_3X_6 , with $X_3 = [0,0]$ and X_6 as given in Lemma 3.

Lemma 5. X'_6 (equivalent to X_{574}) is stationary and given by:

$$X_6' = X_{574} = \left[0, -\frac{Ru\sqrt{u^2 - 3}}{u^2 + 3}\right]$$

<i>Proof.</i> X'_{6} is X_{574} of the reference triangle [10, X(6)]. The latter is the inverse	of
X_{187} with respect to the Brocard circle [10, X(574)]. In turn, X_{187} is the inverse	of
X_6 with respect to the circumcircle. X_6 is stationary in the porism [4]. Carrying of	ut
the inversions in reverse order, and noting that both the circumcircle and Broca	rd
circle are stationary, obtain the claim. See Appendix C for a method to obtain t	he
expression for X_{574} .	

Corollary 4. The Brocard Circle K' of T' is stationary.

This stems from the fact that stationary X_3' and X_6' are antipodes on \mathcal{K}' [19, Brocard Circle].

Corollary 5. X'_{15} and X'_{16} are stationary.

Proof. X'_{15} (resp. X'_{16}) coincide with X_{15} (resp. X_{16}) [10, X(15) and X(16)], shown in Lemma 1 to be stationary.

Corollary 6. The T' family is equibrocardal, i.e., ω' is invariant.

Proof. Plugging invariant X_3', X_6', X_{15}' are stationary in the "combo" (1) of Lemma 5 yields a unique w'.

Let R denote the circumradius of a triangle. After [19, Second Brocard Circle]:

Definition 6 (Second Brocard Circle). Let \mathcal{K}_2 denote the circle centered on X_3 through both Brocard points Ω_1, Ω_2 and with radius $R_2 = R\sqrt{1 - 4\sin^2 \omega}$.

Lemma 6. The second Brocard circle \mathcal{K}'_2 of the T' family is stationary.

Proof. The T' family is inscribed in a fixed circle (i.e., X_3' is stationary and R' is invariant). Since ω' is invariant (Corollary 6), so is R_2' , and the result follows. \square

Corollary 7. The Brocard midpoint X'_{39} of the T' is stationary.

Proof. X_{39} is the inverse of X_6 with respect to \mathcal{K}_2 [10, X(39)]. Since both X'_6 and \mathcal{K}'_2 are stationary (Lemmas 5 and 6), the result follows.

Corollary 8. Ω'_1 , Ω'_2 are stationary.

Proof. These both lie on \mathcal{K}' and their join is perpendicular to the Brocard axis $X_3'X_6'$, intersecting it at X_{39}' [19, Brocard Circle]. Since all stationary, the result follows.

The following results are used to entail Theorem 2.

Lemma 7. X'_6 (equivalent to X_{574}) is interior to the segment X'_3X_6 (equivalent to $X_{182}X_6$).

Proof. Assume X_3 is at the origin. An expression for X_6 was given in Lemma 3 and one for X_6' in Lemma 5. Noting that $X_{182} = \frac{1}{2}X_6$ and $w^2 \geq 3$ (Remark 1) yields the result.

Proposition 3. The Brocard circle K' of T' is contained within its circumcircle, i.e., the Brocard circle K of its reference triangle.

Proof. Since $X_3'X_6'$ is a diameter of \mathcal{K}' , and both are contained within \mathcal{K} (see Lemma 5), the result follows.

Referring to Figure 3:

Theorem 1. The family of second Brocard triangles are 3-periodics in a new Brocard porism specified by:

$$R' = \frac{R\sqrt{w^2 - 3}}{2w}$$

$$X'_3 = [0, -R']$$

$$w' = \frac{w^2 + 3}{2w}$$

$$(a', b') = R' \left(\frac{1}{\sqrt{w'^2 + 1}}, \frac{2}{w'^2 + 1}\right)$$

$$\Omega'_1 = \Omega_2 (R', w') + X'_3$$

$$\Omega'_2 = \Omega_1 (R', w') + X'_3$$

$$X'_{182} = \left[0, -\frac{3R' (w^2 + 1)}{4 w' w}\right]$$

where $w' = \cot \omega'$ and $\Omega_i(R, w)$, i = 1, 2 are as in Proposition 2.

Proof. In a general triangle (see Figure 2), the major (resp. minor) axes of the Brocard Inellipse are oriented along $\Omega_1\Omega_2$ (resp. the Brocard axis X_3X_6) and its center is the Brocard midpoint X_{39} [19, Brocard Inellipse]. Since the Brocard points Ω'_1 , Ω'_2 of T' are stationary (Corollary 8), the center of \mathcal{E}' is stationary center. Since X_3 and X_6 are stationary antipodes of \mathcal{K} , \mathcal{E}' is axis-aligned with \mathcal{E} . Plug invariant R_2 and ω' into the equations in Lemma 2 and obtain invariant (a',b') as in the claim.

Peter Moses let us know that X'_{182} is none other than X_{39498} [13].

Remark 2. The upper vertex of the inellipse of Brocard \mathcal{E}' is at the Brocard midpoint $X_{39} = X'_{39} + [0, b']$.

Corollary 9. The semi-axes of \mathcal{E}' can be expressed in terms of those of \mathcal{E} as follows:

$$[a',b'] = \left[\frac{a\sqrt{a^2 - b^2}}{\sqrt{a^2 + 2b^2}}, \frac{b\sqrt{a^2 - b^2}\sqrt{4a^2 - b^2}}{a^2 + 2b^2} \right]$$

Proof. This follows from Theorem 1 and Lemma 2.

4. An infinite sequence of porisms

Referring to Figure 4:

Theorem 2. Recursive calculation of the second Brocard triangle produces an infinite sequence of Brocard porisms $\mathcal{B}', \mathcal{B}'', \mathcal{B}''', \dots$ such that:

- The isodynamic points are stationary at the original X_{15} and X_{16} .
- The Brocard circle of each new porism is contained within the Brocard circle of its parent, forming an infinite nesting.
- Both the circumradius R and the eccentricity ε of the inellipse decrease monotonically.
- The Brocard angle ω increases monotonically and converges to $\pi/6$ (i.e., triangles approach equilaterals).
- The sequence of porisms converges to X_{15} .

Proof. Corollary 5 entails fixed isodynamic points. Proposition 3 entails Brocard circle infinite nesting. The other results stem from recursive application of relations in Theorem 1. \Box

Defined in [12, p. 78], and cited in [11, P(2)]:

Definition 7 (Beltrami Points). Denoted P_2 and U_2 , these are the inverses with respect to the circumcircle of the Brocard points. They lie on the Beltrami (or Lemoine) axis L_{563} , parallel to a line through the Brocard points [10, Central Lines].

Introduced in [8]:

Definition 8. (Anti second Brocard triangle) Given a triangle T, its anti second Brocard triangle T^* is a triangle whose second Brocard is T.

Proposition 4. Recursive calculation of the anti second Brocard triangle produces an infinite sequence of Brocard porisms \mathcal{B}^* , \mathcal{B}^{***} , \mathcal{B}^{***} , ... such that:

- The isodynamic points remain stationary at the original X_{15} and X_{16} .
- The Brocard circle of each new porism is exterior to the previous one, forming a reverse infinite nesting.
- The sequence of porisms converges to segment P_2U_2 , i.e.
 - The inellipse major (resp. minor) semi-axis converges to $|P_2U_2|$ (resp. 0).
 - The circumradius R monotonically increases and converges to infinity.
 - The Brocard angle ω decreases monotonically to zero.

Proof. The result follows applying Theorem 1 and Propositions 12 and 14 observing that we can invert the process of recurrence taking the sequence of second anti Brocard triangles T^*, T^{**}, \ldots , as isosceles triangles tangent to the Brocard innelipse as shown in Fig. 5.

Definition 9 (Beltrami Circles). Given a triangle, let C_1 (resp. C_2) denote the first (resp. second) Beltrami circle, passing through the first P_2 (resp. second U_2) Beltrami point, containing their circumcircle inverse Ω_1 (resp. Ω_2).

Lemma 8. The the Beltrami circles C_1 and C_2 are centered on

$$P_2, U_2 = \left[\mp \frac{R}{\sqrt{u^2 - 3}}, -\frac{Ru}{\sqrt{u^2 - 3}} \right]$$

Proof. The circumcircle inverse of Ω_1 is $O_1=P_2$ and that of Ω_2 is $O_2=U_2$. Therefore,

$$P_2 = R^2 \frac{\Omega_1}{|\Omega_1|^2}, \quad U_2 = R^2 \frac{\Omega_2}{|\Omega_2|^2}$$

Therefore the result follows from Proposition 2.

Proposition 5. The Beltrami circles intersect at X_{15} and X_{16} and their radii ρ is equal and given by:

$$\rho = \frac{2R}{\sqrt{u^2 - 3}}$$

Moreover, the triangles $X_{15}P_2U_2$ and $X_{16}P_2U_2$ are equilateral.

Proof. Follows from Lemmas 1 and 8.

Theorem 3. The sequence Ω_1 , Ω'_2 , Ω_1'' , Ω_2''' , etc. (resp. Ω_2 , Ω'_1 , Ω''' , Ω_1''') is concyclic on the first (resp. second) Beltrami circle.

Proof. Using Proposition 12, Lemma 9 and Theorem 1 we compute explicitly the sequence of Brocrard points stated. It is straightforward to derive the equation of the circles. They are given by

$$C_1: 4h^2(3d^2 - h^2)(x^2 + y^2) - 8dh^2\zeta x - 4h(3d^2 + h^2)\zeta y + (3d^2 - h^2)\zeta^2 = 0$$

$$C_2: 4h^2(3d^2 - h^2)(x^2 + y^2) + 8dh^2\zeta x - 4h(3d^2 + h^2)\zeta y + (3d^2 - h^2)\zeta^2 = 0$$

where $\zeta = d^2 + h^2$. The centers are

$$O_{1,2} = \left[\pm \frac{d\zeta}{3d^2 - h^2}, \frac{(3d^2 + h^2)\zeta}{2h(3d^2 - h^2)} \right] = \left[\pm \frac{R}{\sqrt{u^2 - 3}}, -\frac{Ruu}{\sqrt{u^2 - 3}} \right]$$

The common radius ρ is given by

$$\rho = \frac{2d\zeta}{3d^2 - h^2} = \frac{2R}{\sqrt{u^2 - 3}}$$

The intersections of C_1 and C_2 are triangle centers X_{15} , X_{16} of Lemma 1.

Using the definition in [19, Isodynamic Points]:

Definition 10. (Apollonius Circles) Given a triangle, there are three circles passing through one vertex and both isodynamic points X_{15} and X_{16} .

Let \mathcal{T} be the upright isosceles 3-periodic with half base d and height h.

Corollary 10. The Beltrami circles are the first and second Apollonius circles of \mathcal{T} . The third Apollonius circle is degenerate and coincides with the Brocard axis.

Proof. The anti-second Brocard \mathcal{T}^* of \mathcal{T} has Brocard points Ω_2^* , Ω_1^* which coincide with vertices B and A of \mathcal{T} . Applying Theorem 3 in reverse direction, Ω_2^* , Ω_1^* will lie each on \mathcal{C}_2 and \mathcal{C}_1 , respectively. Therefore \mathcal{C}_2 (resp. \mathcal{C}_1) passes through vertex B (resp. A) and the two stationary isodynamic points X_{15} , X_{16} (anti-Brocards preserve these). By definition these are the first and second Apollonius circles [19, Isodynamic Points]. The third Apollonius circle contains the two isodynamic points and vertex C of \mathcal{T} . Since these are collinear on the Brocard axis, the circle is a line.

Proposition 6. C_1 and C_2 are perpendicular to each Brocard circle in the sequence.

Proof. It is straightforward to verify the claim for the circumcircle of isosceles triangle \mathcal{T} , given implicitly by

$$x^2 + y^2 - R^2 = 0$$
, $R = \frac{d^2 + h^2}{2h}$.

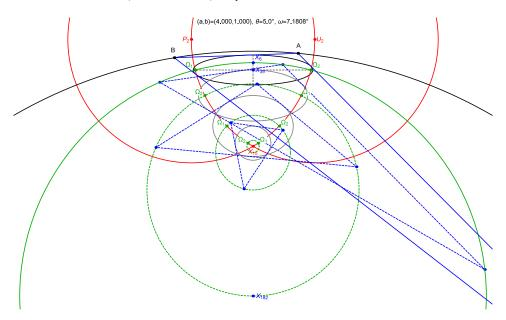


Figure 4. Three iterations of second Brocard triangles (dashed blue), each spawning its own Brocard porism. Successive Brocard points descend in alternate fashion along two circular arcs (red). These intersect at X_{15} and X_{16} (above page, not shown), with centers on the Beltrami points P_2, U_2 . The sequence of Brocard points and porisms converges to the first isodynamic point X_{15} , common to all porisms. At every generation the circumcircle-inellipse pair approaches a shrinking pair of concentric circles (the triangle family approaches equilaterals). Video

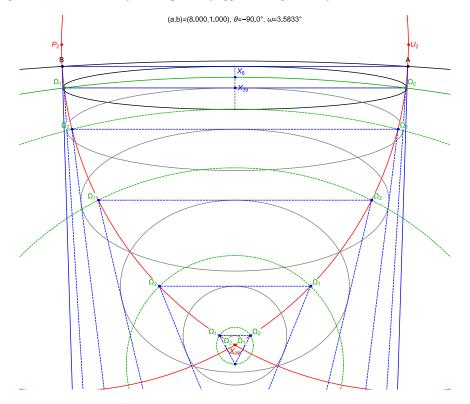


FIGURE 5. Sequence of porisms with successive Brocard points walking along two circular arcs (red) bounded by the Beltrami points P_2, U_2 and X_{15} . For each generation the isosceles $\mathcal T$ 3-periodic is shown (solid blue = first generation, dashed blue = subsequent ones). The bottom vertex is not shown (below the page). The base vertices A, B, or A', B', etc., of a given $\mathcal T$ are the Brocard points of the previous generation. And that their midpoint coincides with the top vertex of the Brocard inellipse.

5. Embedding the discrete sequence of porisms in a continuous family

Consider a family of axis-aligned ellipses \mathcal{E}_t , $0 \le t \le \pi/3$ centered at $O_t = [0, -\sin t]$ with semi-axes a, b given by:

$$a = \frac{\sqrt{2\cos t - 1}}{2}, \quad b = \frac{\sqrt{(2\cos t - 1)(1 - \cos t)}}{\sqrt{2}}$$

Referring to Figure 6(left):

Remark 3. The eccentricity of \mathcal{E}_t is given by $\varepsilon_t = \sqrt{2\cos t - 1}$. The foci $f_{1,t}$ and $f_{2,t}$ lie each on distinct unit-radius circulars arc centered on $\mathcal{C}_1, \mathcal{C}_2 = [0, \mp 1/2]$, respectively. Namely:

$$f_{1,t}, f_{2,t} = \left[\cos t \pm \frac{1}{2}, -\sin t\right]$$

Theorem 4 (Continuous). There is a continuous family of Brocard porisms $\mathcal{B}_t = (\Gamma_t, \mathcal{E}_t)$ whose 1d family of triangles:

• is inscribed in circle Γ_t centered on $X_{3,t}$ with radius R_t given by:

$$X_{3,t} = \left[0, \frac{\sin t}{2(\cos t - 1)}\right], \quad R_t = \sqrt{\frac{2\cos t - 1}{2(1 - \cos t)}}$$

- circumscribes \mathcal{E}_t , its Brocard inellipse (i.e., its Brocard points $\Omega_{1,t}, \Omega_{2,t}$ are $f_{1,t}, f_{2,t}$)
- Has fixed isodynamic points $X_{15,16}$ at $[0, \mp \sqrt{3}/2]$
- Has fixed Brocard angle $\omega_t = t/2$
- Has Brocard circle K_t centered on $X_{182,t} = [0, \frac{\cos t 2}{2 \sin t}]$ with radius $\rho_t = \frac{2 \cos t 1}{2 \sin t}$

Proof. Let \mathcal{T} be the isosceles triangle defined by the vertices $A = f_1$, $B = f_2$ and $C = [0, \frac{\sin t}{2(\cos t - 1)}]$ (t subscripts are omitted). Let vertex C be at the intersection of the line $U_2 f_2$ with the y axis. Applying Lemma 9 to this triangle it follows that:

$$R' = \frac{13 \cos t - 3 \cos 2t - 8}{4 \sin t}, w' = \frac{2 - \cos t + 2}{\sin t}$$

Invert the expressions for R', u' in Theorem 1 to obtain the anti Brocard triangle \mathcal{T}^* of \mathcal{T} , inscribed in Γ_t . By construction, $C = X_3$ of \mathcal{T}^* and the pair $(\mathcal{E}_t, \Gamma_t)$ is a Brocard porism.

Remark 4. Any Brocard porism is a similarity image of a porism B_t defined in Theorem 4.

Referring to Figure 7 (right):

Corollary 11 (Brocard Circle Containment). Let $s, u \in [0, \pi/3]$ and s > u. Then the corresponding Brocard circles $K_s \subset K_u$.

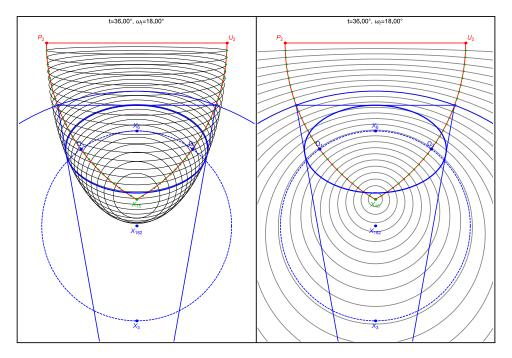


FIGURE 6. Left: A continuous family of inellipses (gray) is shown with foci (green dots) sliding along two 60° circular arcs (red) delimited by P_2, X_{15} and U_2, X_{15} . A particular one $(t=36^\circ)$ is highlighted (thick blue), with foci Ω_1, Ω_2 . A Brocard porism is formed when \mathcal{E}_t is paired with circle Γ_t (blue). An isosceles 3-periodic is shown (blue) interscribed in the pair. Also shown is the fixed Brocard circle (dashed blue). Right: The family of circles Γ_t (gray) is nested and converges to X_{15} . Video

Proof. Combining the the expressions for center and radius of \mathcal{K}_t and in Theorem 4 the claim is true if and only if:

$$\sin(s-u) + \sin u \ge \sin s.$$

where $s, u \in [0, \frac{\pi}{3}]$ with s > u. As the above inequation is equivalent to

$$\sin(s-u)(1-\cos u) + \sin u(1-\cos(s-u)) > 0$$

follows the result. \Box

Theorem 5 (Embedding). The family of second Brocard triangles of \mathcal{B}_t are the 3-periodics of a distinct porism $\mathcal{B}_{t'}$, t' > t, such that:

$$\cot t' = ut' = \frac{4 - 4\cos t + \cos 2t}{4\sin t - \sin 2t} = \frac{u^2 + 3}{2u}$$

Proof. By Theorem 4 the inellipse which yields w_t is given by $t = h(w_t) = \tan^{-1}(\frac{2u_t}{w_t^2-1})$. From Theorem 1 obtain that $w' = g(w_t) = (w_t^2+3)/(2w_t)$. Taking the composition $(h \circ g \circ h^{-1})(t)$ leads to the result.

Proposition 7. The circles K_t are perpendicular to C_1 and C_2

Proof. Let

$$C_{1,2}: \left(x \pm \frac{1}{2}\right)^2 + y^2 - 1 = 0$$

$$K_t: x^2 + \left(y - \frac{\cos t - 2}{2\sin t}\right)^2 - \left(\frac{2\cos t - 1}{2\sin t}\right)^2 = 0$$

The intersection of the circles $C_{1,2}$ and K_t are the points

$$p_{1,\mp} = \left[\mp \frac{3(2\,\cos t - 1)}{2(5 - 4\,\cos t)}, -\frac{3\sin t}{5 - 4\,\cos t}\right], \quad p_{2,\mp} = \left[\mp (\frac{1}{2} - \cos t), \sin t\right]$$

Direct calculations show that $\langle \nabla C(p_{i,\mp}), \nabla K(p_{i,\mp}) \rangle = 0$.

Remark 5. For any B_t , the midpoint X_{187} of P_2U_2 is the inverse with respect to Γ_t of the symmedian point $X_{6,t}$.

Let Z_t denote the lower vertices of \mathcal{E}_t . Setting the derivative of b in Theorem 4 to zero obtain:

Corollary 12. The minor semi-axis b (resp. Z_t) of \mathcal{E}_t reverses direction of motion at $t_b = \cos^{-1}(3/4) \simeq 41.41^{\circ}$ (resp. $t_0 = \tan^{-1}(4/3) \simeq 53.13^{\circ}$). Furthermore $0 \le b \le 1/4$.

Note that the major semi-axis a and the y-coordinate of the upper vertex of \mathcal{E}_t are monotonically decreasing.

Proposition 8. The envelope ξ of the family \mathcal{E}_t is given by:

$$\xi_{1,t}, \xi_{2,t} = \left[\pm \frac{\sqrt{5\cos t - 3}}{2\sqrt{\cos t + 1}}, -\frac{2\sin t}{\cos t + 1} \right]$$

and this is contained in the ellipse given by

$$4x^2 + y^2 - 1 = 0$$

Furthermore, the isodynamic points X_{15} , X_{16} are at its foci.

Proof. The ellipse \mathcal{E}_t is parametrized by

$$\Gamma(u,t) = [a(t)\cos u, b(t)\sin u] + [0, -sin(t)]$$

The envelope is the solution to $\Gamma(u,t) = \Gamma_t(u,t) = 0$ which leads to the claim. \square

Remark 6. At $t > t_0 = \cos^{-1}(\frac{3}{5}) = \tan^{-1}(\frac{4}{3})$ the family \mathcal{E}_t is nested and so the envelope is empty for $t > t_0$. See Fig. 7.

Proposition 9. When $t < \tan^{-1}(\frac{4}{3})$ the Brocard Circle K_t intersects the Brocard inellipse \mathcal{E}_t at its envelope $\xi_{1,t}$ and $\xi_{2,t}$.

Proof. The Brocard circle passes through the point $[0, -\frac{\sin t}{2(1-\cos t)}]$ and it is tangent to the Brocard inellipse at the point [0, -1] when $\tan t = 4/3$.

Proposition 10. The major semi-axis a is concave and monotonically-decreasing with a(0) = 1, $a(\frac{\pi}{3}) = 0$. The minor semi-axis b is concave with a global maximum $\frac{1}{4}$ attained at $t = \cos^{-1}(\frac{3}{4})$ and $b(0) = b(\frac{\pi}{3}) = 0$. The eccentricity $\varepsilon(t) = \frac{c(t)}{a(t)}$ is a concave function with $\varepsilon(0) = 1$, $\varepsilon(\frac{\pi}{3}) = 0$.

Proof. Direct analysis from Theorem 4.

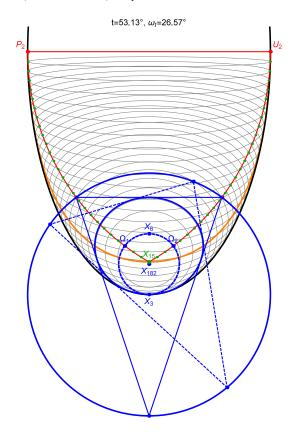


FIGURE 7. The envelope (thick black) of inellipses \mathcal{E}_t (gray) is an ellipse (only bottom half shown) whose foci are the isodynamic points X_{15}, X_{16} common to all families. At $t_0 = \cos^{-1}(3/5)$, the porism is such that the Brocard circle (dashed blue) is tangent to \mathcal{E}_t (solid blue), X_3 is at the envelope's lower vertex, and the lower vertex of \mathcal{E}_t reverses direction of motion. A non-isosceles 3-periodic (dashed blue) is also shown. The locus (orange) of points at which the 3-web formed by the family of inellipses \mathcal{E}_t is perpendicular to the family of Brocard circles K_s (taken as independent families) is a quartic containing the isodynamic and Beltrami points; see Remark 9.

Let $V_l(t)\Gamma(-\frac{\pi}{2},t)=[0,-b(t)-\sin t]$ denote the lower vertex of \mathcal{E}_t .

Corollary 13. $V_l(t)$ moves non-monotonically along the Brocard axis and converges to $X_{15} = [0, -\frac{\sqrt{3}}{2}]$. At $t_0 = \tan^{-1}(\frac{4}{5})$ it attains a global minimum [0, -1].

Proof. Direct analysis from Theorem 4.

Remark 7. At $t = \tan^{-1}(\frac{4}{5})$, $u = \frac{5+\sqrt{41}}{4} \approx 2.851$. At $t = \cos^{-1}(\frac{3}{5})$, u = 2,

Remark 8. The family of ellipses \mathcal{E}_t is defined by the implicit differential equation

$$16x^{2}y^{2} dx^{2} - 8xy (4x^{2} - 1) dx dy + (16x^{4} + 8x^{2} + 4y^{2} - 3) dy^{2} = 0$$

The family of circles \mathcal{K}_t is given by the differential equation

$$8xy \, dx - (4x^2 - 4y^2 + 3)dy = 0$$

Consequently, in the interior of the envelope, the family of circles \mathcal{K}_t and ellipses \mathcal{E}_t define a 3-web [1] which is singular at the coordinate axes and the boundary

of the envelope. The orthogonal family to \mathcal{K}_t is the Apollonian pencil of circles passing through the foci of the envelope. See [1] for the classification of other types of 3-webs defined by circles and ellipses.

Referring to Figure 7:

Remark 9. The families of ellipses \mathcal{E}_t and circles \mathcal{K}_s (where t, s are independent parameters) are orthogonal, if and only if,

$$16x^4 + 8x^2 + 4y^2 - 3 = 0.$$

They are tangent, if and only if, xy = 0.

6. Conclusion

Above we describe various properties of a discrete sequence of Brocard porisms induced by the second Brocard triangle, and how said sequence is embedded in a continuous one. Videos mentioned in the text appear on Table 1.

Exp	Title	Link (youtu.be/)
01	1st, 2nd, 5th, and 7th Brocard triangles	_bK-BCQv24A
	over the Brocard porism	
02	Brocard porism and 2nd Brocard triangle	Wgwh4-neJp4
03	Porism induced by family of 2nd Brocard triangles	MprJtB4UW9s
04	Infinite sequence of Brocard porisms	Z3Y1EbCFbnA
	induced by the second Brocard triangle	
05	Continuous family of Brocard porisms	jY_8zxBljuk

Table 1. Illustrative animations, click on the link to view it on YouTube and/or enter youtu.be/<code> as a URL in your browser, where <code> is the provided string.

We would like to thank Peter Moses for his prompt and invaluable help with dozens of questions related to Brocard geometry, and Daniel Jaud for his generous and precise editorial help. The second author is fellow of CNPq and coordinator of Project PRONEX/ CNPq/ FAPEG 2017 10 26 7000 508.

APPENDIX A. ISOSCELES 3-PERIODIC

Consider an isosceles 3-periodic $\mathcal{T} = ABC$ in the Brocard porism, where AB is tangent to \mathcal{E} at one of its minor vertices. Let |AB| = 2d and the height be h. Let $\zeta = d^2 + h^2$. Let the origin (0,0) be at its circumcenter X_3 . Its vertices will be given by:

$$A = \left[-d, \frac{d^2 - h^2}{2h} \right], \quad B = \left[d, \frac{d^2 - h^2}{2h} \right], \quad \left[0, \frac{\zeta}{2h} \right]$$

Proposition 11. The Brocard porism containing \mathcal{T} as a 3-periodic is defined by the following circumcircle \mathcal{K}_0 and Brocard inellipse \mathcal{E} :

$$\mathcal{K}_0 : x^2 + y^2 - R^2 = 0, \quad R = \frac{\zeta}{2h}$$

$$\mathcal{E} : -64d^2h^4x^2 - 4h^2(9d^2 + h^2)\zeta y^2 + 4h(3d^2 + h^2)(3d^2 - h^2)\zeta y$$

$$- (d^2 - h^2)(9d^2 - h^2)\zeta^2 = 0$$

Proof. The proof follows from \mathcal{T} , and isosceles 3-periodic. Recall that the Brocard inellipse is centered at X_{39} . Its perspector is X_6 , i.e., it will be tangent to \mathcal{T} where cevians through X_6 intersect it; see Figure 2.

Proposition 12. The semi-axes (a,b) of \mathcal{E} are given by:

$$(a,b) = \left(\frac{d\sqrt{\zeta}}{9d^2 + h^2}, \frac{4d^2}{9d^2 + h^2}\right)$$

Furthermore, the Brocard points, located at the foci of \mathcal{E} are given by:

$$\Omega_1, \Omega_2 = \left[\pm \frac{d(3d^2 - h^2)}{9d^2 + h^2}, \frac{9d^4 - h^4}{2h(9d^2 + h^2)} \right]$$

Proof. Follows directly from Proposition 11 computing the semi-axes and foci of the ellipse defined by \mathcal{E} .

Lemma 9.

$$R = \frac{\zeta}{2h}, \quad u = \frac{3d^2 + h^2}{2dh}, \quad \sin \omega = \frac{2dh}{\sqrt{(9d^2 + h^2)\zeta}}$$

Or inversely:

$$d = -\frac{\left(-2 u + \sqrt{u^2 - 3}\right) R}{u^2 + 1}, \quad h = \frac{\left(u^2 + u \sqrt{u^2 - 3} + 3\right) R}{u^2 + 1}$$

Proof. Follows from Propositions 11 and 12.

APPENDIX B. BROCARD PORISM VERTICES

Let d, h be the half base and height of \mathcal{T} , respectively. Let $\zeta = d^2 + h^2$.

Proposition 13. Parametrics for the 3-periodic vertices in terms of t are given by:

$$A = \left[\frac{\zeta}{2h}\cos t, \frac{\zeta}{2h}\sin t\right]$$

$$B = [b_x, b_y]$$

$$b_x = -\frac{\zeta d\left(2dh\cos t + (3d^2 + h^2)\sin t - 3d^2 + h^2\right)}{2dh(3d^2 - h^2)\cos t - (9d^4 - h^4)\sin t + 9d^4 + 2d^2h^2 + h^4}$$

$$(2) \qquad b_y = \frac{\zeta\left(2dh(3d^2 + h^2)\cos t - (9d^4 - 2d^2h^2 + h^4)\sin t + 9d^4 - h^4\right)}{2dh(3d^2 - h^2)\cos t - (9d^4 - h^4)\sin t + 9d^4 + 2d^2h^2 + h^4}$$

$$C = [c_x, c_y]$$

$$c_x = -\frac{\zeta d\left(-2dh\cos t + (3d^2 + h^2)\sin t - 3d^2 + h^2\right)}{(9d^4 - h^4)\sin t + 2dh(3d^2 - h^2)\cos t - 9d^4 - 2d^2h^2 - h^4}$$

$$c_y = \frac{\zeta(2dh(3d^2 + h^2)\cos t + (9d^4 - 2d^2h^2 + h^4)\sin t - 9d^4 + h^4)}{2h(2dh(3d^2 - h^2)\cos t + (9d^4 - h^4)\sin t - 9d^4 - 2d^2h^2 - h^4)}$$

Proof. Given a point $A = R(\cos t, \sin t) \in \mathcal{K}_0$ consider the tangent lines to the Brocard inellipse \mathcal{E} obtained in Proposition 11. The two other intersection points of these lines with \mathcal{K}_0 define the vertices B and C. A long and straightforward calculation with help of a CAS leads to the result stated.

APPENDIX C. FURTHER RELATIONS

Expressions for X_k , k = 6, 15, 16, 39, 574 were given above. They were obtained by starting with the explicit calculation of the triangular center $X_i(t)$ over the family of 3-periodic orbits in the Brocard porism given in Proposition 12.

To this end we make use of the trilinear coordinates f(a, b, c):: of the triangular center X_i [10] and its conversion to Euclidean coordinates expressed by

$$X_i = \frac{s_1 f(s_1, s_2, s_3) A + s_2 f(s_2, s_3, s_1) B + s_3 f(s_3, s_1, s_2) C}{s_1 f(s_1, s_2, s_3) + s_2 f(s_2, s_3, s_1) + s_3 f(s_3, s_1, s_2)}.$$

Here $s_1 = |B - C|$, $s_2 = |C - A|$ and $s_3 = |A - B|$. Obtain the result by simplification via a CA. It is worth mentioning that all triangular centers considered are rational functions of (d, h). Therefore, by Lemma 9 they will be rational functions of $(u, \sqrt{u^2 - 3})$.

Lemma 10. The distance between circumcenter X_3 (respec. X'_3) and symmedian X_6 (respec. X'_6) of T (respec. T') is given by

$$|X_3 - X_6| = \frac{R\sqrt{u^2 - 3}}{u}, \quad |X_3' - X_6'| = \frac{R(u^2 - 3)^{\frac{3}{2}}}{2u(u^2 + 3)}$$

Proof. Consider any triangle with circumradius R and Brocard angle ω . By the construction of the Brocard porism the family has fixed triangular centers X_3 , X_6 , $X_{182} = \frac{1}{2}(X_3 + X_6)$ and X_{574} . As $X_3' = X_{182}$ and $X_6' = X_{574}$ the result follows from Lemmas 4 and 5.

Convergence. Recall that given a map $f: U \to U, U \neq \emptyset$, the positive orbit of point p_0 is the set $O_+(p_0) = \{p_0, f(p_0), f(f(p_0)), \dots, f^n(p_0), \dots\}$. Analogously, when f is invertible, the negative orbit is defined by

$$O_{-}(p_0) = \{p_0, f^{-1}(p_0), f^{-1}(f^{-1}(p_0)), \dots, f^{-n}(p_0), \dots\}.$$

The future (resp. past) of an orbit is the closure of the positive (resp. negative) orbit and is denoted by the ω -limit set $\omega(p_0)$ (resp. α -limit set $\alpha(p_0)$). For an introduction to more properties of these concepts see [5, Chapter 1].

Proposition 14 (Convergence). Let

$$f(R, w) = (p(R, w), q(w)) = \left(\frac{R\sqrt{w^2 - 3}}{2w}, \frac{w^2 + 3}{2w}\right)$$

For any $p_0 = [R_0, u_0]$ with $R_0 > 0$ and $u_0 > \sqrt{3}$, $\omega(p_0)$ is equal to $[0, \sqrt{3}]$ and $\alpha(p_0) = [\infty, \infty]$.

Proof. Define $U = \{(R, u) : u \geq \sqrt{3}\}$. We have that U is invariant by f, i.e., $f(U) \subset U$. We observe that for u > 0, q has a unique fixed point $(0, \sqrt{3})$.

For any $w_0 \ge \sqrt{3}$, $\omega(w_0) = \sqrt{3}$ for q since $q'(\sqrt{3}) = 0 < 1$ (attractor). In fact a global attractor. As $\frac{\sqrt{m^2-3}}{2m} < \frac{1}{2}$ for $m > \sqrt{3}$ and $p(x) < \frac{Rx}{2}$ it follows by a graphic analysis that $\omega(p_0) = [0, \sqrt{3}]$. The inverse of f is given by

$$f^{-1}(R, w) = \left(2w + \sqrt{w^2 - 3}, \frac{\sqrt{2}R\sqrt{y + \sqrt{w^2 - 3}}}{\sqrt[4]{w^2 - 3}}\right)$$

A similar analysis shows that $[0, \sqrt{3}]$ is a repeller of f^{-1} and that the positive orbit of p_0 goes to infinity.

APPENDIX D. TABLE OF SYMBOLS

symbol	meaning	note
T,T'	3-periodic and its 2nd Brocard triangle	
s_1, s_2, s_3	sidelengths of T	
Γ, R	circumcircle and circumradius of T	
\mathcal{E}, a, b	Brocard inellipse and semi-axes	centered on X_{39}
\mathcal{B}	Brocard porism with \mathcal{E} and Γ	
Ω_1,Ω_2	1st and 2nd Brocard points	on foci of $\mathcal E$
ω, uu	Brocard angle and its cotangent	$u = \cot \omega$
\mathcal{K}	Brocard circle	centered on X_{182}
\mathcal{K}_2	second Brocard circle	centered on X_3
\mathcal{T}	isosceles triangle inscribed in Γ	
	whose base is tangent to \mathcal{E} at $(0,b)$	
d, h	half-base and height of \mathcal{T}	
ζ	constant $d^2 + h^2$	
P_2, U_2	1st and 2nd Beltrami points	Γ -inverses of Ω_1, Ω_2
$\mathcal{C}_1,\mathcal{C}_2$	Beltrami Circles	centered on $P_2, U_2,$
		contain X_{15} and X_{16}
X_3	circumcenter (at origin)	$X_3 = [0, 0]$
X_6	symmedian point	
X_{13}, X_{14}	isogonic points	
X_{15}, X_{16}	isodynamic points	
X_{39}	Brocard midpoint	
X_{182}	center of K	midpoint of X_3X_6
X_{187}	Midpoint of Beltrami points	
X_{574}	X_6 of T'	\mathcal{K} -inverse of X_{187}
X_{39498}	X_{182} of T'	

Table 2. Symbols used. Primed symbols in the text refer to the second Brocard triangle.

References

- [1] Akopyan, A. (2018). 3-webs generated by confocal conics and circles. *Geom. Dedicata*, 194: 55-64. https://doi.org/10.1007/s10711-017-0265-6. 15, 16
- [2] Akopyan, A. V., Zaslavsky, A. A. (2007). Geometry of Conics. Providence, RI: Amer. Math. Soc. 3
- [3] Bradley, C. (2011). The geometry of the Brocard axis and associated conics. http://people.bath.ac.uk/masgcs/Article116.pdf. CJB/2011/170. 3
- [4] Bradley, C., Smith, G. (2007). On a construction of Hagge. Forum Geometricorum, 7: 231—247. http://forumgeom.fau.edu/FG2007volume7/FG200730.pdf. 2, 4, 5, 7
- [5] Devaney, R. L. (2003). An introduction to chaotic dynamical systems. Studies in Nonlinearity. Westview Press, Boulder, CO. Reprint of the second (1989) edition. 18
- [6] Garcia, R., Reznik, D. (2020). Loci of the brocard points over selected triangle families. https://arxiv.org/abs/2009.08561. ArXiv:2009.08561.

- [7] Gibert, B. (2020). Brocard triangles and related cubics. https://bernard-gibert.pagesperso-orange.fr/gloss/brocardtriangles.html. 2, 6
- [8] Gibert, B. (2020). Brocard triangles and related cubics. https://bernard-gibert.pagesperso-orange.fr/gloss/anti-brocardtria.html.9
- [9] Johnson, R. A. (1960). Advanced Euclidean Geometry. New York, NY: Dover, 2nd ed. bit.ly/33cbrvd. Editor John W. Young. 3
- [10] Kimberling, C. (2019). Encyclopedia of triangle centers. faculty.evansville.edu/ck6/encyclopedia/ETC.html. 3, 4, 5, 7, 9, 18
- [11] Kimberling, C. (2020). Bicentric pairs. bit.ly/2Svh9Dr. 3, 9
- [12] Morley, F., Morley, F. V. (1954). Inversive Geometry. Chelsea. 9
- [13] Moses, P. (2020). Family of triangles with fixed Brocard points. Private Communication. 8
- [14] Odehnal, B. (2011). Poristic loci of triangle centers. J. Geom. Graph., 15(1): 45-67. 3
- [15] Pamfilos, P. (2020). Triangles sharing their euler circle and circumcircle. *International Journal of Geometry*, 9(1): 5-24. ijgeometry.com/wp-content/uploads/2020/03/1.-5-24.pdf. 3
- [16] Reznik, D., Garcia, R. (2020). Related by similarity II: Poncelet 3-periodics in the homothetic pair and the Brocard porism. arXiv:2009.07647. 3
- [17] Reznik, D., Garcia, R., Koiller, J. (2019). Can the elliptic billiard still surprise us? Math Intelligencer, 42. rdcu.be/b2cg1. 3
- [18] Shail, R. (1996). Some properties of Brocard points. The Mathematical Gazette, 80(489): $485\text{--}491.\ 5$
- [19] Weisstein, E. (2019). Mathworld. MathWorld-A Wolfram Web Resource. mathworld.wolfram.com. 1, 2, 3, 4, 5, 7, 8, 10